PHYSICAL REVIEW A **70**, 032508 (2004)

Density-functional theory in one dimension for contact-interacting fermions

R. J. Magyar
Department of Physics and Astronomy, Rutgers University, 136 Frelinghuysen Road, Piscataway, New Jersey 08854-8019, USA

K. Burke
Department of Chemistry and Chemical Biology, Rutgers University, 610 Taylor Road, Piscataway, New Jersey 08854-8019, USA

(Received 4 February 2004; published 21 September 2004)

A density-functional theory is developed for fermions in one dimension, interacting via a δ function. Such systems provide a natural testing ground for questions of principle, as the local-density approximation should be highly accurate since for this interaction type the exchange contribution to the local-density approximation is intrinsically self-interaction-free. The exact-exchange contribution to the total energy is a local functional of the density. A local-density approximation for correlation is obtained using perturbation theory and Bethe ansatz results for the one-dimensional contact-interacting uniform Fermi gas. The ground-state energies are calculated for two finite systems, the analogs of helium and of Hooke's atom. The local-density approximation is shown to be excellent as expected.

DOI: 10.1103/PhysRevA.70.032508 PACS number(s): 31.15.Ew, 71.10.−w, 71.15.Mb

I. INTRODUCTION

Density-functional theory (DFT) is a rigorous reinterpretation of the quantum many-body problem in which the basic object uniquely characterizing a system is the density $n(x)$ rather than the many-body wave function. This view is particularly suited to practical calculations, and DFT has been applied successfully to solids and molecules for quite some time [1]. Researchers typically focus on Coulomb-interacting fermions in three dimensions, but the Hohenberg-Kohn theorem [2–5] upon which DFT is based holds for any interaction and in any spatial dimension. We consider the contact or δ-function interaction between fermions in one spatial dimension,

$$v_{\mathrm{int}}(x_i - x_j) = \lambda\,\delta(x_i - x_j), \tag{1}$$

where x_i and x_j represent the spatial coordinates of the fermions, $\delta(x)$ is the Dirac delta function, and λ is the interaction strength. The fermions have two spin states, up and down. The δ-function potential is a one-dimensional analog to the Coulomb one as it scales in a similar fashion, $v_{\mathrm{int}}(ax)=v_{\mathrm{int}}(x)/a$, and its solutions satisfy the energetically important particle-particle cusp condition [6,7]. However, it differs in that it is short ranged. There is no simple equivalence between λ and e^2, the Coulomb-interaction strength, although λ can be related to a scattering length [8].

One-dimensional model interactions are important for several reasons. Perhaps most obviously, they are useful in mathematical and statistical physics [9–12] to illustrate problems and concepts from three-dimensional physics that are sometimes hard to conceptualize due to the number of degrees of freedom. However, our primary motivation is to use this one-dimensional model to understand and improve density-functional theory. Many of the known formal properties of the exchange-correlation functional are true in this case. These properties include behavior under uniform coordinate scaling [13], the virial theorem, and inequalities due to the variational principle. That properties of the theory still hold should prove extremely useful in exploring time-dependent density-functional theory [14,15], where formal properties are still being investigated. Because the interaction is not the Coulomb one, the unknown exchange-correlation functional will, of course, differ. The local-density approximation (LDA) should be extremely accurate in this case because exchange is treated exactly for this interaction, and there is no exchange self-interaction error. Another reason is that a contact interaction samples only the on-top value of the exchange-correlation hole, and the local-density approximation is known to reproduce this value accurately [16]. The self-interaction-corrected LDA is highly accurate for the ground-state energies of isolated atoms [17,18]. The difference here is that the self-interaction is handled exactly within the local-density formalism and no special corrections are needed. Our LDA could be used to study the one-dimensional analog of stretched H_2 to identify whether the proper description of dissociation into individual atoms depends on the long-ranged Coulomb interaction or is due to symmetry considerations alone. Another interesting system on which to use one-dimensional DFT is the one-dimensional solid. This δ-function interaction has already been used to study problems in DFT [19,20] but without the inclusion of any correlation effects, which are known to be important in one-dimensional systems. An earlier treatment including correlation effects can be found in Ref. [21]. Using DFT to study alternate interactions is not new; for example, Capelle and co-workers have used a similar approach on the Hubbard model [22,23].

It has been suggested that the δ-function model should give a good representation of the physics of one-dimensional fermions in certain experimental contexts [24–28]. Since one-dimensional systems are analytically, or at least computationally, manageable, the exact results are useful to examine situations when standard techniques fail. For example, the one-dimensional analog of helium can be examined in detail near the critical point of ionization when the nuclear attraction and interaction repulsion are comparable. This sort of analysis is demanding for real systems, and finite-size

1050-2947/2004/70(3)/032508(8)/$22.50

scaling and infinite-dimensional approaches are necessary [29–32]. Carefully understanding how systems ionize and how electronic structure methods reproduce this critical phenomenon is useful for many chemical problems. We will examine this limit in detail in future work and present only the most basic results here.

Throughout, we assume that our one-dimensional fermions have the same mass as electrons, and we use atomic units ($e^2=\hbar=m_e=1$) so that all energies are in hartrees and all lengths in Bohr radii.

II. EXACT-EXCHANGE FUNCTIONAL DENSITY-FUNCTIONAL THEORY

In this section, we see how the contact interaction affects the total energy to first order in λ. First-order interaction theory is traditionally called the Hartree-Fock approximation, but here, the first-order interaction energy depends explicitly on the density so that, for this particular interaction, the Hartree-Fock approximation is equivalent to exact-exchange DFT. Consequently, exchange is treated exactly within the local-density approximation for this interaction.

According to density-functional theory [2–5], the ground-state total energy is a functional of the particle density and the local magnetization,

$$\zeta(x) = \frac{n_\uparrow(x) - n_\downarrow(x)}{n_\uparrow(x) + n_\downarrow(x)}, \tag{2}$$

where $n_\uparrow$ and $n_\downarrow$ are the densities of up and down spins. The total ground-state energy can be decomposed as follows:

$$E[n,\zeta] = T_S[n,\zeta] + U_H[n] + E_{XC}[n,\zeta] + \int dx v_{ext}(x) n(x) \tag{3}$$

in a one-dimensional space where $U_H[n]$ is the exactly known Hartree or classical density-density interaction contribution, $v_{ext}(x)$ is the given external potential, $T_S[n,\zeta]$ is the exactly known kinetic energy of noninteracting fermions at a given density, and $E_{XC}[n,\zeta]$ is the unknown exchange-correlation energy. The density is found by studying the Kohn-Sham (KS) system, the noninteracting counterpart to the physical system [33]. The Kohn-Sham equation is

$$\left(-\frac{1}{2}\nabla^2 + v_{S,\sigma}([n,\zeta];x)\right)\phi_{i,\sigma}(x) = \epsilon_{i,\sigma}\phi_{i,\sigma}(x) \tag{4}$$

where $\phi_{i,\sigma}(x)$ is the ith KS orbital for spin type σ, $\epsilon_{i,\sigma}$ is the KS eigenvalue, and $v_{S,\sigma}(x)$ is the KS potential for spin type σ. The Kohn-Sham potential is a functional derivative of the energy functionals,

$$v_{S,\sigma}(x) = v_{ext}(x) + \frac{\delta U_H[n]}{\delta n_\sigma(x)} + \frac{\delta E_{XC}[n,\zeta]}{\delta n_\sigma(x)}, \tag{5}$$

where $n_\sigma(x)$ is the σ spin density. The spin density is obtained from the occupied orbitals,

$$n_\sigma(x) = \sum_{i,\text{occ.}} |\phi_{i,\sigma}(x)|^2. \tag{6}$$

Because of the antisymmetry of the wave function under particle interchange, fermions with like spins do not experience the contact interaction. Only opposite spins interact directly.

The Hartree contribution depends only on the total particle density and is independent of how up and down fermions are distributed:

$$U_H[n] = \frac{\lambda}{2}\int dx dx' n(x)\delta(x-x')n(x') = \frac{\lambda}{2}\int dx n^2(x). \tag{7}$$

There is overcounting here because like spins do not interact, and the exchange term must cancel these spurious like-spin interactions. The exact-exchange term is

$$E_X[n,\zeta] = -\frac{\lambda}{2}\int dx n(x)^2[1+\zeta(x)^2]/2. \tag{8}$$

Equations (7) and (8) follow immediately after substituting the δ-function interaction into the usual Hartree and Fock terms. Note that for a one-fermion system we have $E_X[n,|\zeta|=1] = -U_H[n]$ and contact-interacting exact exchange is self-interaction-free.

III. LOCAL-DENSITY CORRELATION FUNCTIONAL FROM THE ONE-DIMENSIONAL CONTACT-INTERACTING UNIFORM FERMI GAS (DELTIUM)

In order to obtain a local-density correlation functional, we review the one-dimensional unpolarized Fermi gas, which we call deltium. This Fermi gas plays the role of the uniform electron gas in Coulomb-interacting DFT. While the Coulomb-interacting Fermi gas is a Fermi liquid, the one-dimensional δ-function-interacting analog is a Luttinger liquid [34]. The Hamiltonian is

$$\hat{H} = -\frac{1}{2}\sum_i^N \frac{d^2}{dx_i^2} + \lambda\sum_{i<j}\delta(x_i - x_j). \tag{9}$$

The solution must be antisymmetric under particle interchange and satisfy periodic boundary conditions on a ring of circumference L. This system has been examined previously [8,35,36]. Because the wave function is antisymmetric under particle interchange, the fully polarized gas is not affected by the interaction. We consider the correlation in detail for only the fully unpolarized gas. Since $\zeta=0$ in the unpolarized case, we will suppress it except when needed.

The energy per particle of the noninteracting uniform gas is purely kinetic:

$$t(n) = \frac{\pi^2}{24}n^2. \tag{10}$$

When interactions are present, the total energy per particle is

$$\epsilon(n) = t(n) + \epsilon_{\mathrm{H}}(n) + \epsilon_{\mathrm{X}}(n) + \epsilon_{\mathrm{C}}(n), \tag{11}$$

where $\epsilon_{\mathrm{H}}(n)=\lambda n/2$ is the Hartree energy per particle, $\epsilon_{\mathrm{X}}(n) = -\lambda n/4$ is the exchange energy per particle, and $\epsilon_{\mathrm{C}}(n)$ is the correlation energy per particle. It is useful to define the following two terms. Kineticlike means that the energy per particle is proportional to n^2, like the noninteracting kinetic energy. Hartree-like means that the energy per particle is proportional to n, like the Hartree energy.

The ground-state energy per particle for deltium, Eq. (9), can be found via Bethe ansatz methods [37–41], whereby the uniform unpolarized Fermi gas problem can be recast as a set of integral equations [42]:

$$\tau(y) = \frac{1}{2\pi} + \frac{2}{\pi}\int_{-\infty}^{\infty} d\Lambda \frac{\lambda\sigma(\Lambda)}{\lambda^2 + 4(y-\Lambda)^2} \tag{12}$$

and

$$\sigma(\Lambda) = \frac{1}{2\lambda}\int_{-k_{\mathrm{max}}}^{k_{\mathrm{max}}} dy\ \mathrm{sech}[\pi(y-\Lambda)/\lambda]\tau(y), \tag{13}$$

where τ is the number of occupied states per wave-vector label y, and σ is the number of occupied down-spin states per a different wave-vector label Λ. In the high-density limit, $k_{\mathrm{max}}=\pi n/2$, and in the low-density limit, $k_{\mathrm{max}}=\pi n$. Equations (12) and (13) must be solved self-consistently for τ and σ at a chosen value of k_{max} to obtain the ground-state energy. In order to do this, the integrals are transformed to the interval $[-1,1]$, and integrated using six-point quadrature rules with 400 mesh points. The density is

$$n = \int_{-k_{\mathrm{max}}}^{k_{\mathrm{max}}} dy\tau(y), \tag{14}$$

and the total energy per particle is

$$\epsilon = \frac{1}{2n}\int_{-k_{\mathrm{max}}}^{k_{\mathrm{max}}} dyy^2\tau(y). \tag{15}$$

The correlation energy per particle for a wide range of densities can, in the spirit of three-dimensional DFT, be parametrized for practical calculations. We consider both the high- and low-density limits analytically and numerically. Since we are concerned with parametrizing the correlation energy, we subtract out the known kinetic, Hartree, and exchange contributions.

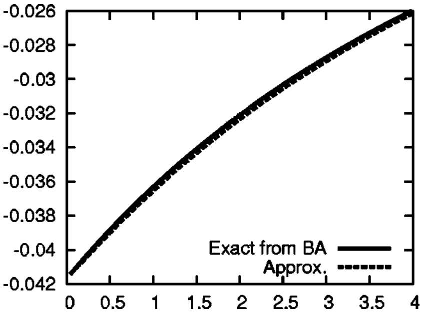

FIG. 1. Correlation energy per particle in atomic units for deltium, the one-dimensional uniform contact-interacting ($\lambda=1$) Fermi gas, in the high-density limit. The solid line is the exact result calculated from the solutions of the Bethem ansatz integral equations. The long-dashed line is the simple LDA given by Eq. (20).

The low-density limit is the large-λ limit. In this limit, the opposite-spin fermions repel each other so strongly that the interaction mimics Fermi antisymmetrization. Thus, the interaction energy per particle is kineticlike. This means that the first term for the correlation energy must cancel the Hartree and exchange energies, and the next term in the correlation energy must be kineticlike. The correlation energy per particle is

$$\epsilon_{\mathrm{C}}(n) = -\frac{\lambda}{4}n + b_1 n^2 - \frac{b_2}{\lambda}n^3 + \mathcal{O}\left(\frac{n^4}{\lambda^2}\right) \tag{16}$$

with $b_1=\pi^2/8$ and $b_2=4.56$. The first term in Eq. (16) exactly cancels the Hartree and exchange energies, and the next, b_1, provides the kineticlike contribution to the energy. We determine the coefficient b_2 from numerical analysis of the Bethe ansatz results at $\lambda=1$. Specifically, we subtract the known contributions from $\epsilon(n)$, divide by n^3, and plot the result as a function of n. The extrapolated intercept at $n=0$ is b_2.

In the high-density limit, the interaction is perturbation-like and the correlation energy per particle approaches a constant:

$$\epsilon_{\mathrm{C}}(n) = -c_1\lambda^2 + c_2\lambda^3/n + \mathcal{O}\left(\frac{\lambda^4}{n^2}\right) \tag{17}$$

with $c_1=1/24$ and $c_2=0.006\,170$. The first term, c_1, is found using perturbation theory in the Appendix. We determine c_2 from numerical analysis of the Bethe ansatz results by subtracting the known contributions from $\epsilon(n)$, multiplying by n, plotting the result as a function of $1/n$, and extrapolating to the origin using a fourth-order polynomial. The correlation energy per particle of the uniform gas approaches a finite value as $n\to\infty$, in contrast to jellium, because the contact interaction is short ranged.

A [2,2] Padé parametrization of the correlation energy per particle is

$$\epsilon_{\mathrm{C}}^{\mathrm{unif}}(n) \approx \left(\frac{an^2 + bn + c}{n^2 + dn + e}\right) \tag{18}$$

with $a=-c_1=-1/24$, $b=-0.004\,361\,43$, $c=0$, $d=0.252\,758$, and $e=0.017\,445\,7$. Note that c is zero because the correlation energy per particle vanishes in the low-density limit. This approximation gives the first and second terms c_1 and c_2 of the high-density limit correctly. In the low-density limit, this approximation cancels the Hartree-exchange term and gives the b_1 coefficient. The parametrization of ϵ_{C}, the correlation energy per particle, has a maximum error of 0.7% and is highly accurate for the important high-density regions. As shown in Figs. 1 and 2, the parametrization is almost

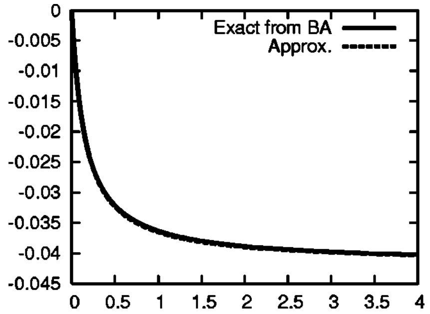

FIG. 2. The same as Fig. 1 but for the low-density limit.

indistinguishable from the exact numerical result. Equation (18) is valid at $\lambda=1$ but can be generalized to arbitrary λ according to scaling rules: $\epsilon_{\mathrm{C}}^{\mathrm{unif},\lambda}(n)=\lambda^2\epsilon_{\mathrm{C}}^{\mathrm{unif}}(n/\lambda)$.

For the fully polarized case ($|\zeta|=1$), the interaction does not contribute to the energy and

$$E_{\mathrm{C}}^{\mathrm{LDA}}[n,|\zeta|=1]=0. \tag{19}$$

We can combine these results and construct a local-density correlation energy functional:

$$\begin{aligned} E_{\mathrm{C}}^{\mathrm{LDA}}[n,\zeta] &= \int dx n(x)\epsilon_{\mathrm{C}}^{\mathrm{unif}}(n(x))f(\zeta(x)) \\ &\approx \int dx\left(\frac{an(x)^3+bn(x)^2}{n(x)^2+dn(x)+e}\right)f(\zeta(x)). \end{aligned} \tag{20}$$

A simple suggestion for $f(\zeta)$ which gives both polarized ($|\zeta|=1$) and unpolarized ($\zeta=0$) limits exactly is

$$f(\zeta)=1-\zeta^2, \tag{21}$$

which is the ζ dependence of U_{H} plus E_{X}. We stress that the local-density correlation-energy functional Eq. (20) is self-interaction-free for a one-particle system.

IV. THE ONE-DIMENSIONAL CONTACT-INTERACTING ANALOG OF THE HELIUM ATOM (DIRACIUM)

In order to assess the usefulness of this local approximation to handle one-dimensional problems, we start with perhaps the most difficult test case, a completely nonuniform system, diracium. This is the one-dimensional analog of helium with the traditional Coulomb terms replaced by δ functions. The system is described by the Hamiltonian

$$\hat{H}=-\frac{1}{2}\frac{d^2}{dx_1^2}-\frac{1}{2}\frac{d^2}{dx_2^2}-Z\delta(x_1)-Z\delta(x_2)+\lambda\delta(x_1-x_2) \tag{22}$$

and the eigenvalue equation

$$\hat{H}\Psi_{\sigma\sigma'}(x_1,x_2)=E\Psi_{\sigma\sigma'}(x_1,x_2), \tag{23}$$

where x_1 and x_2 are the positions of the fermions, σ and σ' are the spinlike labels of the fermions, Z is the magnitude of the external potential, and Ψ is an antisymmetric Fermi wave function which vanishes as $x\rightarrow\infty$. The ground state is a spin singlet ($\zeta=0$).

First, we solve the model analytically within the exact-exchange approximation. Then we introduce our local-density approximation to the exchange-correlation energy. Finally, we present the exact energy eigenvalues.

With the exact-exchange functional Eq. (8) and no functional for correlation, the Kohn-Sham single-orbital equation is

$$-\frac{1}{2}\frac{d^2}{d^2x}\phi(x)-Z\delta(x)\phi(x)+\lambda|\phi(x)|^2\phi(x)=\epsilon_{\mathrm{KS}}\phi(x). \tag{24}$$

Equation (24) can be solved using elementary techniques. The resulting eigenvalue is

$$\epsilon_{\mathrm{KS}}=-\frac{1}{2}\left(Z-\frac{1}{2}\lambda\right)^2, \tag{25}$$

and the Kohn-Sham orbital [43] is

$$\phi(x)=\frac{1}{\sqrt{\lambda}}\left(Z-\frac{1}{2}\lambda\right)\mathrm{csch}\left[\left(Z-\frac{1}{2}\lambda\right)|x|+\alpha\right] \tag{26}$$

with

$$\alpha=\mathrm{arccoth}\left(\frac{Z}{Z-\frac{1}{2}\lambda}\right). \tag{27}$$

This is unbound at $Z<\frac{1}{2}\lambda$. The calculated total energy is not just the sum of the occupied KS orbital eigenvalues; rather, it is

$$\begin{aligned} E[n] &= \sum_{\mathrm{occ}}\epsilon_{\mathrm{KS}}+U_{\mathrm{H}}[n]+E_{\mathrm{XC}}[n,\zeta]-\int dxv_{\mathrm{H}}([n,\zeta];x)n(x) \\ &\quad -\int dxv_{\mathrm{XC}}([n,\zeta];x)n(x), \end{aligned} \tag{28}$$

or explicitly

$$E_{\mathrm{EXX}}=-Z^2+\frac{Z\lambda}{2}-\frac{\lambda^2}{12}. \tag{29}$$

Next, we solve the KS equation using the local-density approximation to the correlation. The LDA KS equation is

$$\begin{aligned} &-\frac{1}{2}\frac{d^2}{d^2x}\phi(x)-Z\delta(x)\phi(x)+\lambda|\phi(x)|^2\phi(x) \\ &\quad +v_{\mathrm{C}}([n,\zeta=0];x)\phi(x)=\epsilon_{\mathrm{KS}}\phi(x) \end{aligned} \tag{30}$$

with

$$v_{\mathrm{C}}([n,\zeta=0];x)=\left(1-\frac{b}{b+an(x)}+\frac{2e+dn(x)}{n(x)^2+dn(x)+e}\right)\epsilon_{\mathrm{C}}(x). \tag{31}$$

Equation (30) is solved numerically to self-consistency cycle via the shooting method.

The exact ground-state energies were obtained previously by Rosenthal [44] by transforming to momentum space and reducing the problem to the solution of a one-dimensional integral equation. While this method converges quickly to

TABLE I. Total ground-state energy for diracium (in hartrees) and errors (in millihartrees) of various approximations with $\lambda = 1$. The exact results are from a numerical solution of the problem as outlined by Ref. [44]; the second-order perturbation values are also given in the same reference. The EXX and LDA results are from a self-consistent calculation using the exact-exchange functional Eq. (8) and the LDA functional Eq. (20), respectively. $Z_{\mathrm{crit}} = 0.377\,115$ is the critical value at which the system ionizes [44].

Z	Exact	ΔLDA	Δ EXX	Δ Perturbation theory
Z_{crit}	−0.070276	−45	not bound	46
0.5	−0.129281	−12	not bound	34
1	−0.647225	−3.3	−64	16
2	−3.155390	−1.0	−72	7.4
4	−14.159190	0.7	−76	3.6
8	−60.161010	1.8	−78	1.7
100	−9950.1630	3.2	−80	−0.2

the exact energy eigenvalue, it is not well suited to giving real space wave functions and densities. Instead, we take the calculated eigenvalue E as input and reduce the eigenvalue problem Eq. (22) to a differential equation. The differential equation can then be converted to an integral equation using Green's function techniques:

$$\begin{aligned}\Psi(x,y) = {} & \frac{Z}{\pi}\int_{-\infty}^{\infty} dx' K_0\left(\sqrt{-2E}\sqrt{(x-x')^2+y^2}\right)\Psi(x',0) \\ & + \frac{Z}{\pi}\int_{-\infty}^{\infty} dx' K_0\left(\sqrt{-2E}\sqrt{x^2+(y-x')^2}\right)\Psi(x',0) \\ & - \frac{\lambda}{\pi}\int_{-\infty}^{\infty} dx' K_0\left(\sqrt{-2E}\sqrt{(x-x')^2+(y-x')^2}\right)\Psi(x',x'),\end{aligned} \tag{32}$$

where E is the ground-state energy and K_0 is the zeroth-order modified Bessel function and is the Green's function for this particular two-dimensional equation. We have dropped the spin labels in this case since the exact ground state is a spin singlet. By setting y equal to x and then 0, we can arrive at a set of two coupled integral equations which can be solved self-consistently. Note that, although the Bessel function has a divergence, the integral is finite. Once $\Psi(x,0)$ and $\Psi(x,x)$ are known, we can construct the wave function at any point in space. If the input E is exact, then solution of this equation yields the exact ground-state wave function.

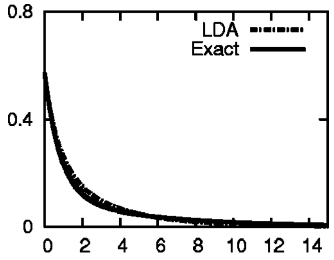

FIG. 3. Comparison of the self-consistent LDA density in atomic units (dashed line) with the exact (solid line) for $\lambda = 1$ and $Z = 0.5$. This is an extreme case where the exact exchange no longer binds.

In Table I, we see that the LDA is much more accurate than the EXX functional. Second-order perturbation theory is more accurate only for $Z \geqslant 7$, but that is at a much larger computational cost since the second-order contribution requires calculation of the entire spectrum of unoccupied orbitals. The LDA remains bound and gives a reasonable result (within a factor of 3) even at the critical potential strength Z_{crit}. In Fig. 3, we see that the LDA gives a qualitatively correct density for $Z = 1/2$ where the EXX result is no longer even bound.

Figure 4 shows that the LDA gives highly accurate correlation energies for the nonperturbative regime when Z is small. In the other extreme, the exact result approaches the second-order perturbation theory value, and the LDA is overcorrelated, as will be discussed later.

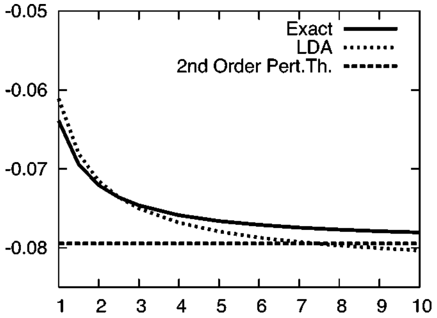

FIG. 4. Correlation energy in atomic units for diracium, the one-dimensional analog of helium ($\lambda = 1$). The solid line is the exact result, the short-dashed line is the LDA result, and the long-dashed line is the second-order perturbation theory result. Note that we extract the correlation energy approximately by subtracting the self-consistent exact-exchange total energy from the exact total energy. The exact-exchange density becomes an unreliable approximation to the exact density as Z decreases and at $Z = 1/2$ the density is even qualitatively wrong as the self-consistent exact-exchange solution is no longer bound. Therefore, we terminate the plot at $Z = 1$ where we expect the self-consistent exact-exchange density to be an accurate representation of the exact density.

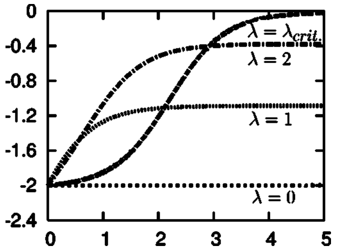

FIG. 5. The behavior of the density in atomic units for diracium ($Z=1$) at various interaction strengths λ. We plot $d\ln n(x)/dx$ to highlight the asymptotic behavior of the density. For $\lambda > \lambda_{\mathrm{crit}}$, the system is ionized.

There exist standard theorems about the decay of the density away from the attractive nuclear potential in the three-dimensional Coulomb-interacting case [45]. For example,

$$n(r) \rightarrow e^{-2\alpha r} \tag{33}$$

as $r \rightarrow \infty$ where $\alpha = \sqrt{2I}$. This theorem also holds for our one-dimensional model with $r=|x|$. There is much interest in critical values of Z at which an atom can no longer bind its outermost electron [29–31]. Understanding this limit yields information on the existence of negative ions. A most interesting question is this: As $Z \rightarrow Z_{\mathrm{crit}}$ and $I \rightarrow 0$, how does the density decay? We study this directly in our one-dimensional example by varying λ and keeping Z fixed at 1. For large enough λ, the system will ionize. Note that $\lambda_{\mathrm{crit}} = 1/Z_{\mathrm{crit}}$. Figure 5 shows $d\ln n/dx$ as $\lambda \rightarrow 1/Z_{\mathrm{crit}}$ for $Z=1$.

The second-order perturbation theory result for diracium differs from the high-density LDA result. The second-order perturbation theory result is

$$E_{\mathrm{C}} = (-3/8 + 2/3\pi + 1/12)\lambda^2 = -0.0795\lambda^2. \tag{34}$$

The first two terms are the exact contribution to the total energy to order λ^2 [46]. From this, we subtract the final term, which is the exchange contribution via the self-consistent density. The high-density LDA correlation result is

$$E_{\mathrm{C}} = -\lambda^2/12 = -0.083\,333\lambda^2. \tag{35}$$

The LDA correctly scales to a constant in the high-density limit in contrast to three-dimensional Coulomb DFT [47] (see Fig. 3).

Another interesting quantity to consider as the particle-particle interaction grows stronger is the interaction energy or the expectation value of $v_{\mathrm{int}}(x_i - x_j)$. For small λ, the interaction energy grows in magnitude as λ grows, but at $\lambda \approx 0.9$, this trend reverses. For $\lambda \geqslant \lambda_{\mathrm{crit}}$, the system is ionized, so that the interaction energy is zero. Figure 6 shows that, as $\lambda \rightarrow \lambda_{\mathrm{crit}}$ from below, the approach to this discontinuity is linear. This information is valuable in studying the approach to ionization, and may also be true for real two-electron ions.

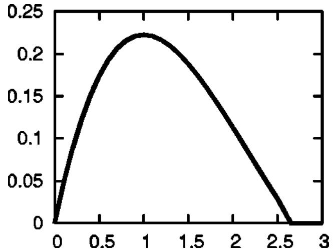

FIG. 6. The expectation value of the interaction in atomic units at various interaction strengths λ. Beyond $\lambda = \lambda_{\mathrm{crit}}(2.6517)$, the system is ionized and the interaction energy vanishes.

TABLE II. Total ground-state energy for the contact-interacting Hooke's atom (in hartrees) and errors (in millihartrees) of various approximations with $\lambda=1$. Exact result is from a numerical solution of Eqs. (37) and (38). EXX is exact exchange. The LDA is according to the parametrization Eq. (20).

ω	Exact	Δ EXX	ΔLDA
0.001	0.001950	−6.1	−0.08
0.01	0.018510	−12.6	−0.7
0.1	0.161410	−48.2	−3.5
1	1.306750	−72.2	−6.3
10	11.157330	−82.9	−6.4
100	103.881057	−86.5	−5.7

V. δ-FUNCTION-INTERACTING HOOKE'S ATOM

Another test of this one-dimensional LDA is the analog to Hooke's atom [48],

$$\hat{H} = -\frac{1}{2}\frac{d^2}{dx_1^2} - \frac{1}{2}\frac{d^2}{dx_2^2} + \frac{1}{2}\omega^2 x_1^2 + \frac{1}{2}\omega^2 x_2^2 + \lambda\,\delta(x_1 - x_2), \tag{36}$$

where ω determines the strength of the harmonic well potential. This model has been used to model one-dimensional quantum dots [24], and its excitations have been studied using time-dependent DFT [49]. The exact wave function is given in terms of Whittaker functions and confluent hypergeometric functions [24]. The total energy is

$$E = \frac{1}{2}\omega + \varepsilon \tag{37}$$

with ϵ obtained from the solution of [24,49]

$$2\sqrt{2\omega}\,\Gamma\left(-\frac{\epsilon}{2\omega} + \frac{3}{4}\right)\Big/\Gamma\left(-\frac{\epsilon}{2\omega} + \frac{2}{4}\right) = -\lambda. \tag{38}$$

In Table II, we see that the LDA greatly improves over the exact-exchange formalism for all values of ω.

In the high-density or weak-coupling ($\lambda \rightarrow 0$) limit, this system behaves similarly to diracium, described above. The total energy can be described perturbatively

$$E = \omega + \lambda c_1 \omega^{1/2} + \lambda^2 c_2 + \cdots, \tag{39}$$

where $c_1 = 1/\sqrt{2\pi} = 0.399$ and $c_2 = \left[\gamma + \psi^{(0)}\left(\tfrac{1}{2}\right)\right]/4\pi = -0.110\,318$ with γ being the Euler constant and $\psi^{(0)}$ the zeroth-order polygamma function. The λ^2 term above is the high-density limit of the correlation energy plus an exchange contribution. In DFT, the exchange contribution is the first-order contribution in $\tilde{\lambda}$ where $\tilde{\lambda}$ is the coupling constant for a fixed fermion density. Here, λ is the interaction strength, and when it varies so does the ground-state density. This means that in a self-consistent calculation exchange will contribute to second order in λ to the total energy. We saw this in Eq. (29) for diracium. The same is true here. As for diracium, the LDA is very accurate in the high-density limit. In order to properly compared the LDA correlation energy with the exact one, we need to extract the exact density.

Since Hooke's atom stays bound for arbitrarily weak ω, we can see how well our LDA describes the low-density limit. The low-density limit is particularly challenging for Coulomb-interacting functionals [50] because of the strong correlation. The LDA and generalized gradient approximations behave qualitatively correctly but often err by as much as a factor of 2 for the exchange-correlation energy. For Hooke's atom, the exact result for the total energy in the strong-coupling limit is

$$E = 2\omega. \tag{40}$$

The low-density limit is related to the large-coupling-constant limit. As $\lambda \to \infty$, the lowest-energy solution in the relative coordinate $|x_1 - x_2|$ is simply the first noninteracting excited state because inserting a node at $x_1 = x_2$ minimizes the interaction energy. We find that the LDA is remarkably accurate in this regime, so the errors in Coulomb-interacting DFT can be ascribed to the long-range interaction.

The energy in this regime becomes kineticlike. The exact-exchange functional is Hartree-like and will fail to capture the proper energetics. The LDA, however, cancels the Hartree-like exchange contributions and is kineticlike. In the low-density regime the density is close to uniform locally, so we expect the energy per particle to be similar to that of low-density deltium. This is in fact the case and is reflected by the high accuracy of the LDA in the low-density regime.

VI. CONCLUSION

In this paper, we examined a one-dimensional density-functional theory of contact-in-teracting fermions. We noted that exact exchange is an explicit density functional and developed a local-density approximation for correlation. We applied these functionals successfully to two simple models, demonstrating the high accuracy of the LDA here. Although the LDA is highly accurate in these cases, it is not exact. This result is consistent with the observation in Ref. [51] that the LDA is not exact in the short-wavelength limit.

This model interaction and LDA can be used to illustrate and explore problems in DFT. Examples include ground-state symmetry problems in stretched H_2 and the interacting-fermion one-dimensional solid (a generalized Kronig-Penney model) as a model band-gap problem. This δ-function interaction has already been used in scattering problems and in pedagogy, and we hope that our local-density correlation functional finds fruitful applications in these areas as well.

ACKNOWLEDGMENTS

We would like to thank C. Rosenthal for discussions. This work was supported by the National Science Foundation under Grant No. CHE-9875091 and the Department of Energy under Grant No. DE-FG02-01ER45928.

APPENDIX

Here, we find the high-density limit of the correlation energy per particle for deltium using perturbation theory and the diagrammatic approach in momentum space [52]. The Fourier transform of the interaction potential is

$$V(q) = \frac{\lambda}{L}\int_{-L}^{L} dx\,\delta(x)e^{iqx} = \frac{\lambda}{L} \tag{A1}$$

where L is the length between the periodic boundaries. As noted earlier, like-spin fermions will not interact via the δ function; this means that only vertices that connect opposite spins will enter into the perturbative series. This is a tremendous simplification as many diagrams will cancel. A further simplification is that the interaction is independent of the momentum transfer q.

To first order, only the Hartree diagram between opposite spins contributes to the total energy. This is the first diagram in Fig. 7. Evaluation does not require integration over internal momentum. The loop integrals have prefactors of $L^2/4\pi^2$, and integration over the loops results in a factor of $2k_F = \pi n$ each, where $k_F = \pi n/2$ is the Fermi momentum of noninteracting deltium. The symmetry factor of $1/2$ is canceled by a sum over the two possible pairs of spin. The final energy per particle is obtained by dividing by N, the total particle number. We find

$$N\epsilon_{HX} = \frac{\lambda}{L}\left(\frac{L^2}{4\pi^2}\right)\pi^2 n^2 \to \epsilon_{HX} = \lambda\frac{n}{4}. \tag{A2}$$

To second order, only one more diagram contributes. This is the two-bubble diagram shown second in Fig. 7. From the standard rules of perturbation theory,

$$N\epsilon_C^{(2)} = -\frac{\lambda^2}{L^2}\frac{L^3}{8\pi^3}\int_{-\infty}^{\infty} dq \int_{-k_f}^{k_f} dk_1 \int_{-k_f}^{k_f} dk_2 \frac{1}{q(q+k_1-k_2)} \tag{A3}$$

where $|k_1+q| > 1$ and $|k_2 - q| > 1$, k_1 and k_2 are particle momenta, and q is the momentum transfer. The limits of integration and constraint inequalities ensure that particles have less momentum than the Fermi momentum, and holes have

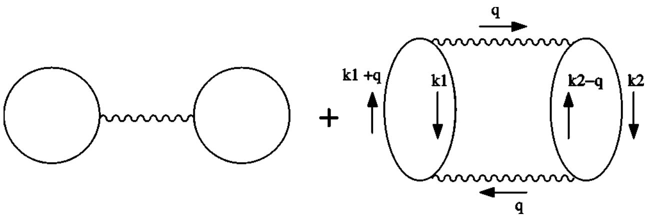

FIG. 7. First- and second-order contributions to the interaction energy. Spin labels are omitted but the two loops in each diagram must have opposite spins. q is the momentum transfer, k_1 and k_2 label particle momenta, and k_1+q and k_2-q label hole momenta.

higher momentum than the Fermi momentum. Once again, the sum over the two possible spin arrangements cancels the symmetry factor of 1/2. To solve Eq. (A3) exactly, we rescale as follows: $q=k_F x$, $k_1=k_F y$, and $k_2=k_F z$. After some algebra, we find the correlation energy per particle:

$$\epsilon_C^{(2)} = -\frac{\lambda^2}{8\pi^3}\left(\frac{L}{N}\right)\left(\frac{\pi n}{2}\right)\mathcal{I} = -\frac{\lambda^2}{24} \tag{A4}$$

using the quadrature result

$$\mathcal{I} = 2\int_2^{\infty} dx \int_{-1}^{1} dy \int_{-1}^{1} dz \frac{1}{x(x+y-z)} + 2\int_0^{2} dx \int_{1-x}^{1} dy \int_{-1}^{-1+x} dz \frac{1}{x(x+y-z)} = \frac{2\pi^2}{3}. \tag{A5}$$

[1] R.O. Jones and O. Gunnarson, Rev. Mod. Phys. **61**, 689 (1989).

[2] P. Hohenberg and W. Kohn, Phys. Rev. **136**, B864 (1964).

[3] U. von Barth and L. Hedin, J. Phys. C **5**, 1629 (1972).

[4] K. Capelle and G. Vignale, Phys. Rev. Lett. **86**, 5546 (2001).

[5] H. Eschrig and W. Pickett, Solid State Commun. **118**, 123 (2001).

[6] J.C. Kimball, Phys. Rev. A **7**, 1648 (1973).

[7] E.R. Davidson, *Reduced Density Matrices in Quantum Chemistry* (Academic Press, New York, 1976).

[8] A. Gold, Phys. Rev. B **55**, 9470 (1997).

[9] M. Takahashi, *Thermodynamics of One-Dimensional Solvable Models* (Cambridge University Press, Cambridge, England, 1999).

[10] *The Many-Body Problem: An Encyclopedia of Exactly Solved Models in One Dimension*, 2nd ed., edited by D. Mattis (World Scientific, Singapore, 1994).

[11] P. Schlottmann, Int. J. Mod. Phys. B **11**, 355 (1997).

[12] J. Voit, Rep. Prog. Phys. **58**, 977 (1995).

[13] M. Levy and J.P. Perdew, Phys. Rev. A **32**, 2010 (1985).

[14] E. Runge and E.K. U. Gross, Phys. Rev. Lett. **52**, 997 (1984).

[15] N.T. Maitra, K. Burke, H. Appel, E.K. U. Gross, and R. van Leeuwen, in *Reviews in Modern Quantum Chemistry: A Celebration of the Contributions of R.G.Parr*, edited by K. D. Sen (World Scientific, Singapore, 2001), pp. 1186—1225.

[16] K. Burke, J.P. Perdew, and M. Ernzerhof, J. Chem. Phys. **109**, 3760 (1998).

[17] J. P. Perdew and A. Zunger, Phys. Rev. B **23**, 5048 (1981).

[18] S. Goedecker and C.J. Umrigar, Phys. Rev. A **55**, 1765 (1997).

[19] N.T. Maitra, A. Wasserman, and K. Burke, in *Electron Correlations and Materials Properties 2*, edited by A. Gonis, N. Kioussis, and M. Ciftan (Kluwer/Plenum, Dordrecht, 2003).

[20] A.W. Overhauser, Phys. Rev. Lett. **4**, 462 (1960).

[21] K. Capelle and L.N. Oliveira, Phys. Rev. B **61**, 15228 (2000).

[22] K. Capelle, N.A. Lima, M.F. Silva, and L.N. Oliveira, in *The Fundamentals of Density Matrix and Density Functional Theory in Atoms, Molecules, and Solids*, edited by N. Gidopoulos and S. Wilson (Kluwer, Dordrecht, 2003).

[23] N.A. Lima, M.F. Silva, L.N. Oliveira, and K. Capelle, Phys. Rev. Lett. **90**, 146402 (2003).

[24] Th. Busch and C. Huyel, J. Phys. B **36**, 2553 (2003).

[25] C.L. Kane and Matthew P. A. Fisher, Phys. Rev. Lett. **68**, 1220 (1992).

[26] D. Alan Tennant, RogerA. Cowley, StephenE. Nagler, and AlexeiM. Tsvelik, Phys. Rev. B **52**, 13368 (1995).

[27] D.C. Dender, P.R. Hammar, Daniel H. Reich, C. Broholm, and G. Aeppli, Phys. Rev. Lett. **79**, 1750 (1997).

[28] S. Qin, M. Fabrizio, L. Yu, M. Oshikawa, and I. Affleck, Phys. Rev. B **56**, 9766 (1997).

[29] Sabre Kais and Pablo Serra, Int. Rev. Phys. Chem. **19**, 97 (2000).

[30] Pablo Serra and Sabre Kais, Phys. Rev. Lett. **77**, 466 (1996).

[31] Pablo Serra and Sabre Kais, Phys. Rev. A **55**, 238 (1996).

[32] Pablo Serra, Juan Pablo Neirotti, and Sabre Kais, Phys. Rev. Lett. **80**, 5293 (1998).

[33] W. Kohn and L.J. Sham, Phys. Rev. **140**, A1133 (1965).

[34] P. Schlottmann, J. Phys.: Condens. Matter **6**, 1359 (1994).

[35] F.D. Buzatu, Phys. Rev. B **55**, 2114 (1997).

[36] S. Nagano and K.S. Singwi, Phys. Rev. B **27**, 6732 (1983).

[37] E.H. Lieb and W. Liniger, Phys. Rev. **130**, 1605 (1963).

[38] M. Gaudin, Phys. Lett. **24A**, 55 (1967).

[39] M. Flicker and E.H. Lieb, Phys. Rev. **161**, 179 (1967).

[40] C.N. Yang, Phys. Rev. Lett. **19**, 1312 (1967).

[41] A.D. Jannussis, Phys. Rev. Lett. **21**, 523 (1968).

[42] W.I. Friesen and B. Bergersen, J. Phys. C **13**, 6627 (1980).

[43] E.H. Lieb, J.P. Solovej, and J. Yngvason, Phys. Rev. Lett. **69**, 749 (1992).

[44] C. Rosenthal, J. Chem. Phys. **55**, 2474 (1971).

[45] O.J. Heilmann and E.H. Lieb, Phys. Rev. A **52**, 3628 (1995).

[46] R.J. White and F.H. Stillinger, Phys. Rev. A **3**, 1521 (1971).

[47] A. Görling and M. Levy, Phys. Rev. B **47**, 13105 (1993).

[48] M. Taut, Phys. Rev. A **48**, 3561 (1993).

[49] N.T. Maitra, F. Zhang, R.J. Cave, and K. Burke, J. Chem. Phys. **120**, 5932 (2004).

[50] H.B. Shore, E. Zaremba, J.H. Rose, and L. Sander, Phys. Rev. B **18**, 6506 (1978).

[51] K. Burke, J.P. Perdew, and D.C. Langreth, Phys. Rev. Lett. **73**, 1283 (1994).

[52] R.D. Mattuck, *A Guide to Feynman Diagrams in the Many-Body Problem* (Dover, New York, 1976).